



Study on Removal of Thallium from Wastewater by Chitosan/Fly Ash Composite Adsorbent

Li Hai-hua*†, Chen Jie*, Hua Yong-peng**, Yan Shao-feng**, E. Zheng-yang* and Su Hang*

*Faculty of Environmental and Municipal Engineering, North China University of Water Resources and Electric Power, Zhengzhou 450011, China

**Henan Academy of Environmental Protection Sciences, Zhengzhou 450011, China

†Corresponding author: Li Hai-hua

Nat. Env. & Poll. Tech.

Website: www.neptjournal.com

Received: 11-06-2019

Accepted: 24-07-2019

Key Words:

Thallium
Chitosan
Fly ash
Wastewater

ABSTRACT

Thallium (Tl) is a kind of emerging contaminant with strong toxicity. In this study, a low-cost, renewable, biologically low-toxic and environmentally friendly fly ash/chitosan (FACS) composite adsorption material was synthesized by combining the characteristics of chitosan and fly ash to remove thallium from wastewater. SEM, FTIR and XRD analyses showed that the adsorbent mainly contained silicate compounds, and the surface of the particles contained a large number of micro porous structures. The adsorption process was rapid, reaching the adsorption equilibrium after 60min. When the pH value was 8, FACS had the best adsorption effect on Tl, which was not conducive to the adsorption of Tl in either strong acid or strong base environment. The co-existence of Fe³⁺ and Mn²⁺ could facilitate the adsorption of Tl by FACS. The adsorption isotherm data were better fitted for the Freundlich model, while the Second-order kinetic model was more suitable for describing the kinetic data. Since the main chemical bond composition and chemical groups of FACS would not change after the adsorption of Tl, the removal rate of Tl was still high when it was reused after desorption. Because of its simple operation, low cost and reusability, FACS is considered to have certain potential in the removal of Tl from wastewater.

INTRODUCTION

Thallium (Tl) is a rare heavy metal element in the third main group, but it is widely found in nature (Liu et al. 2017, Xiao et al. 2012). In the past few decades, very low concentrations of thallium were contained in uncontaminated natural freshwater (Del-valls et al. 1999, Cheam et al. 1995). However, due to the human activities such as mining, smelting and coal burning, the content of thallium in natural water is rising in recent years (Zhang et al. 2018). Once, as it was an unconventional test indicator in water, soil and solid waste, the problem of thallium pollution has been ignored. In fact, thallium, a highly toxic heavy metal contaminant, is one of the most toxic metals that poison mammals, and it is even more toxic than many of the highly regarded heavy metals such as mercury, cadmium, lead and zinc (Zhang et al. 2018, Wick et al. 2018, Xiao et al. 2018). Considering the toxicity and environmental pollution, Tl has been listed as a priority pollutant by many official agencies (Liu et al. 2017). Therefore, the removal of thallium from wastewater seems to be particularly important.

So far, several technologies for removing thallium from water or wastewater have been reported, such as chemical precipitation (Liu et al. 2017), ion exchange (Li et

al. 2017), solvent extraction (Rajesh & Subramanian 2006), adsorption (Birungi & Chirwa 2015, Huangfu et al. 2017) and biological methods (Saljooghi et al. 2011, Zolgharnein et al. 2011). Among these methods, adsorption is highly regarded by the researchers because of its high removal efficiency and simple operation. Varieties of materials such as titanium peroxide (Zhang et al. 2018), manganese dioxide (Huangfu et al. 2017), multiwalled carbon nanotubes (Pu et al. 2013), modified anion exchange resins (Li et al. 2017), Sawdust (Memon et al. 2008), fungi (Chen et al. 2018), and algae (Birungi & Chirwa 2015) have been used as adsorbents to remove Tl from wastewater. Unfortunately, among these adsorbents, some are expensive, some cannot be reused, and others are hardly to obtain. As a result, it is urgent to develop a highly efficient adsorbent that is not only inexpensive but also easy to prepare and regenerate to remove Tl from wastewater.

Fly ash (FA), is a kind of industrial waste formed by high-temperature calcination of pulverized coal. Due to its high porosity, large specific surface area and high adsorption activity, more and more people use it to make adsorption for environmental pollutant treatment (Ge et al. 2018). Chitosan (CS) is a product of the deacetylation of

chitin, and it is widely found in nature. Due to its biodegradability, biocompatibility and renewability, chitosan has been recognized as one of the most promising materials for adsorbents (Fan et al. 2012, Kuroiwa et al. 2017). So far, there have been some researches on fly ash/chitosan composite adsorbents. For example, Wen et al. (2011) used chitosan to coat fly ash to prepare a composite biosorbent and then studied the structural characteristics of the adsorbent and the adsorption effect on Cr(VI) in aqueous solution. Pan et al. (2011) prepared chitosan/fly-ash-cenospheres/ γ -Fe₂O₃ magnetic composites by using micro-emulsion process and explored the removal of bisphenol A and 2,4,6-trichlorobenzene from aqueous solution. Yang et al. (2018) synthesized a new macromolecular xanthogen chitosan heavy metal chelation flocculant to treat wastewater containing Cu²⁺. Rathinam et al. (2018) used synthetic chitosan-lysozyme biocomposites to effectively remove dyes and heavy metals from aqueous solutions. However, there is no research on the use of fly ash/chitosan (FACS) composite adsorbents to remove TI from polluted water. So, the purpose of this research was to synthesize fly ash/chitosan (FACS) composite adsorbent and analyse its characteristics by FIRT, SEM and XRD. The effects of the adsorbent on TI were investigated by changing some influencing factors, such as pH of the solution, reaction time, the amount of adsorbent, coexisting ions and rotational speed. The data of adsorption kinetics was explored. Meanwhile, we used two isotherm models to evaluate this adsorbent. Finally, we tested it for its reproducibility.

MATERIALS AND METHODS

Materials

The chitosan used in this study was purchased from Beijing Solarbio Science & Technology Co. Ltd. Fly ash was purchased from Lanke Water Purification Materials Co., Ltd. All the chemicals used in the study were of analytical grade. TI single element standard solution, which is an international standard substance, was purchased from Steel Research Institute of Iron and Steel Testing Technology Co., Ltd.

PHS-3C pH meter manufactured by Shanghai Yidian Scientific Instrument Co., Ltd. was used to measure the pH of the solution. The atomic absorption spectrum of the sample was measured by using a PinAAcle 900Z atomic absorption spectrometer manufactured by Perkin Elmer. The sample was oscillated with zh-d type all-temperature oscillator produced by Jintan Jingda Instrument Manufacturing Co., Ltd. Scanning electron microscopy analysis of the samples, Fourier infrared spectroscopy and X-ray diffraction analysis were performed by qualified units.

Preparation of Composite Adsorbent

The chitosan/fly ash (FACS) was thoroughly mixed at a mass ratio of 1:12.5, and then glacial acetic acid was added at a concentration of 4%, wherein the mass ratio of glacial acetic acid to the mixture was 3:5. All the materials were mixed and stirred thoroughly, and then prepared into small particles with a particle size of 1~3mm. After this, small particles were dried to obtain the FACS composite adsorbent. It should be noted that the co-existing ions were not added during the experiment, and the composite adsorbent adsorbing the aqueous solution only containing TI (I) was represented by TFACS. Similarly, the composite adsorbent, which adsorbed the solution containing only the coexisting ion Fe³⁺, was represented by Fe-FACS, the composite adsorbent adsorbing the solution in which Mn²⁺ ions were added was represented by Mn-FACS, and the composite adsorbent adsorbing the solution in which the Fe³⁺/Mn²⁺ mixed ion was added was represented by FM-FACS.

Characterization of Adsorbents

The FACS of unabsorbed heavy metal and the composite materials TFACS, Fe-FACS, Mn-FACS and FM-FACS adsorbed with heavy metals were scanned by scanning electron microscope to observe the structural characteristics. The infrared spectra of the composite TFACS, Fe-FACS, Mn-FACS and FM-FACS were tested by FTIR spectroscopy and the changes of covalent bonds and corresponding groups were observed. The XRD patterns of the FACS composite adsorbent were obtained by X-ray diffraction in the range of $2\theta = 10\sim 80^\circ$, and the diffraction peaks in the spectrum were observed to analyse the crystallinity of FACS.

Experimental Design

The experimental parameters such as pH, contact time, the amount of adsorbent, presence of coexisting ions and rotational speed on the removal of TI were studied in a batch mode of operations. 80mL of TI-containing wastewater with an initial concentration of 0.01mg/L was added into a 250 mL volumetric flask, and the experimental conditions were changed to carry out a batch adsorption experiment. All the experiments were carried out under constant temperature conditions. After the desired time, the supernatant was taken to determine the content of thallium in the wastewater.

Adsorption Kinetics

The adsorption rate is a crucial indicator to evaluate the applicability of the given adsorbent for practical application because of its decisive role on the initial investment. The kinetics of adsorption that describes the solute uptake

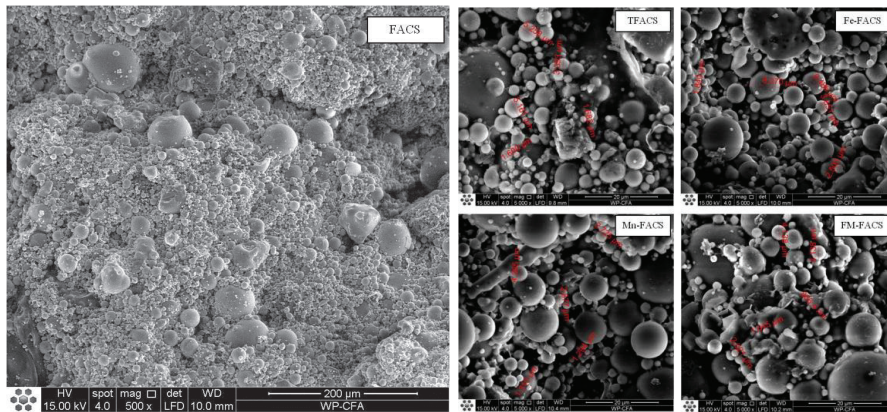


Fig. 1: The SEM pictures of various FACS.

rate is one of the most important characteristics that define the efficiency of adsorption (Wan et al. 2014, Xiong et al. 2013). The First-order kinetics model is expressed as the follow equation (Keskinkan et al. 2004):

$$\ln(q_e - q_t) = \ln q_e - k_1 t$$

The Second-order kinetics model is expressed as the following equation (Xiong et al. 2013):

$$\frac{t}{q_t} = \frac{1}{k_2 q_e^2} + \frac{t}{q_e}$$

Where, q_e and q_t are the amounts of Tl(I) adsorbed at equilibrium and at time t , respectively.

Adsorption Isotherms

The adsorption isotherm describes the relationship between the adsorption capacity of adsorbent and the equilibrium concentration of adsorbent, and it plays an important role in understanding the adsorption process (Zhang et al. 2008, Li et al. 2018, Tran et al. 2017). Langmuir and Freundlich are two different isothermal adsorption models. The Langmuir model was established based on the assumption that the adsorbent surface was uniform, and the equation was expressed as (Rahmani et al. 2010, Saad et al. 2018):

$$\frac{C_e}{q_e} = \frac{C_e}{q_0} + \frac{1}{bq_0} \quad \dots(3)$$

Where, C_e is the equilibrium concentration of the solution (mg/L), q_e is the amount of heavy metal adsorbed per unit weight of adsorbent at a specified equilibrium (mg/g), q_0 is the saturated adsorption capacity of monomolecular coverage (mg/g), and b is the adsorption rate constant (L/mg).

The Freundlich equation is an empirical equation for describing the surface heterogeneity of adsorbent (Rahmani et al. 2010, Saad et al. 2018) and given as:

$$\ln q_e = \ln k + \frac{1}{n} \ln C_e \quad \dots(4)$$

Where, C_e is the mass concentration of solute at adsorption equilibrium (mg/L), q_e is the equilibrium adsorption quantity (mg/g), k is the Freundlich constant representing the adsorption capacity (mg/g), and n is a constant representing the adsorption intensity.

RESULTS AND DISCUSSION

Characterization of Adsorbents

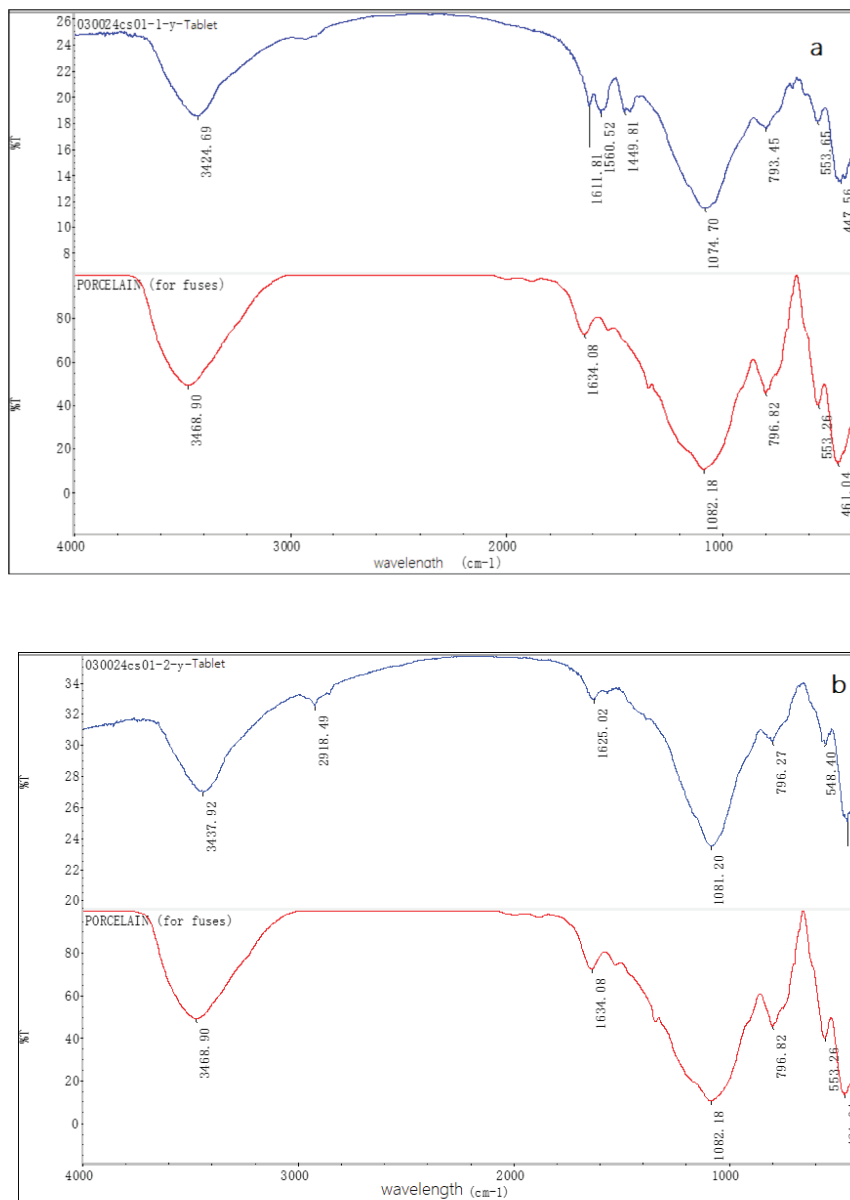
In order to observe the morphological changes before and after adsorption of FACS composite adsorption materials, the original FACS and the TFACS, Fe-FACS, Mn-FACS and FM-FACS after adsorption were analysed by scanning electron microscopy, and the results are presented in Fig. 1. It can be seen from Fig. 1 that the surface of the FACS particles contained a large number of microporous structures, and there was more particulate matter in the outer layer. The foremost reason is that the FACS consists of a large amount of fly ash particles, and the particles are connected to each other. It indicates that the colloidal solution formed by the dissolution of chitosan was solidified by fly ash to make both of them fully mixed together to form FACS particles. The SEM scan showed that the FACS particles were filled with micropores after the adsorption. Minimum particle sizes of TFACS, Fe-FACS, Mn-FACS and FM-FACS particles were 1.600 μ m, 1.840 μ m, 1.294 μ m and 0.866 μ m, respectively. It is not hard to find that, compared with Fe-FACS, Mn-FACS and FM-FACS, TFACS with only TI adsorption had

more pore structures, indicating that the surface porosity of adsorbent particles had a small change when only TI was adsorbed. The main reason for the above phenomenon is that in the presence of co-existing ions Fe^{3+} , Mn^{2+} and $\text{Fe}^{3+}/\text{Mn}^{2+}$, FACS also adsorbed Fe^{3+} and Mn^{2+} to some extent in the process of adsorbing TI, so the surface porosity of Fe-FACS, Mn-FACS and FM-FACS particles decreased significantly compared to FACS.

Fourier infrared spectroscopy was used to detect and analyse FACS, TFACS, Fe-FACS, Mn-FACS and FM-FACS re-

spectively, in order to understand the molecular structure and group changes in FACS composite adsorbents before and after adsorption. The Fourier infrared spectrum is shown in Fig. 2.

As can be seen from Fig. 2a, in the FACS spectrum, the chemical absorption peak of the O-H bond was at 3424.69 cm^{-1} , the characteristic absorption peak of C-H bond was at $1611.81 \text{ cm}^{-1} \sim 1449.81 \text{ cm}^{-1}$, and the characteristic infrared absorption peak of Si-O bond was at 1074.70 cm^{-1} . In combination with the FTIR diagram to which silicate



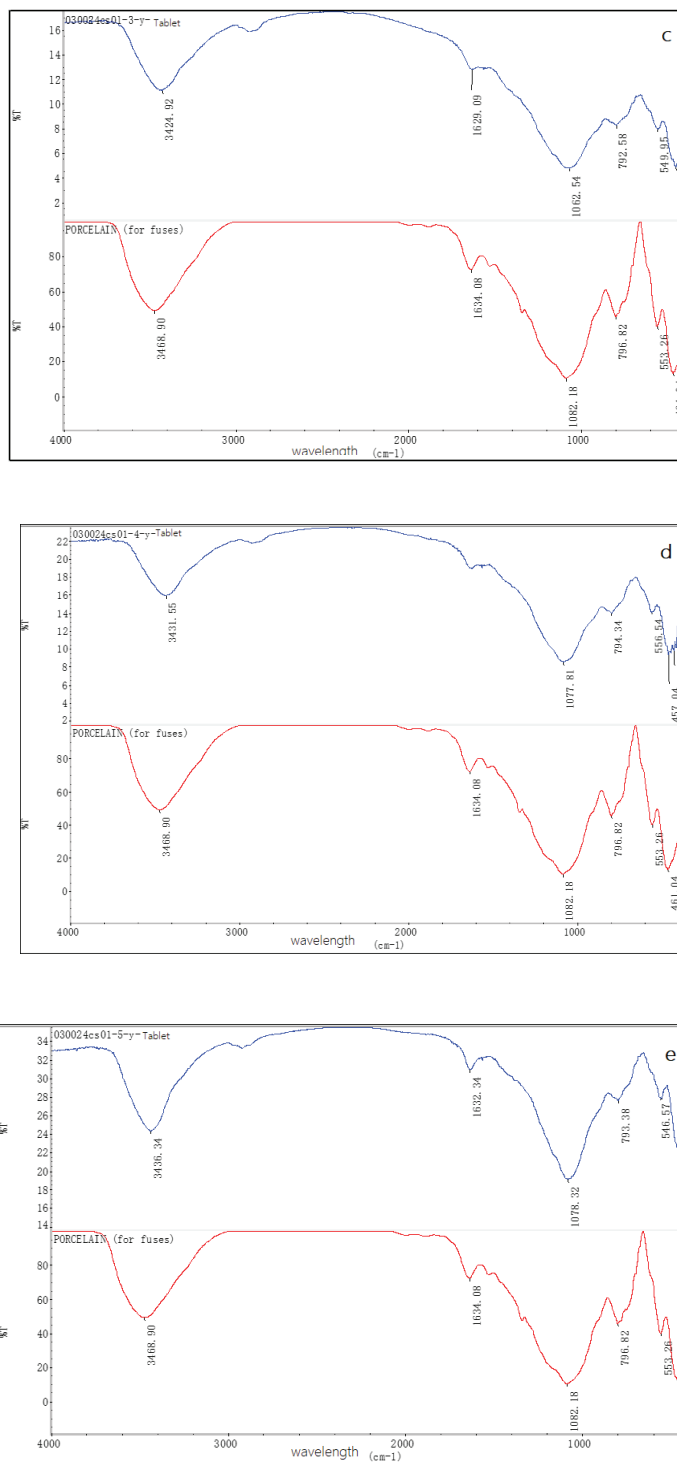


Fig. 2: The FTIR pictures of FACS.

compounds were matched, it can be seen that the FACS mainly consisted of silicon-containing compound.

It can be found from Fig. 2b that in the TFACS spectrum, the stretching vibration peak of the O-H bond was at 3437.92 cm^{-1} , C-H key characteristic absorption peak was at 1625.02 cm^{-1} , and Si-O key characteristic in absorption peak was at 1081.20 cm^{-1} . At the same time, in combination with the FTIR diagram to which silicate compounds were matched, it can be seen that TFACS mainly consisted of silicon-containing compounds, and a special vibration peak was generated at 2918.49 cm^{-1} after the adsorption of thallium.

As shown in Fig. 2c, in the Fe-FACS spectrum, the characteristic chemical absorption peak of the O-H bond was at 3424.92 cm^{-1} , the characteristic absorption peak of the C-H bond was at 1629.09 cm^{-1} , and the characteristic infrared absorption peak of Si-O bond was at 1062.54 cm^{-1} . Matching the FTIR map, it can be seen that the Fe-FACS mainly consisted of silicon-containing compounds.

As described in Fig. 2d, in the Mn-FACS spectrum, the characteristic chemical absorption peak of the O-H bond was at 3431.55 cm^{-1} , the characteristic absorption peak of the C-H bond was at 1634.08 cm^{-1} , and the characteristic infrared absorption peak of Si-O bond was at 1077.81 cm^{-1} .

Then based on the matching of silicate compounds with FTIR diagram, it can be considered that the Mn-FACS mainly consisted of silicon-containing compounds.

According to Fig. 2e, in the FM-FACS spectrum, the stretching vibration peak of the O-H bond was at 3463.34 cm^{-1} , the characteristic absorption peak of C-H bond was at 1632.34 cm^{-1} , and the Si-O bond characteristic infrared absorption peak was at 1078.32 cm^{-1} . Compared to silicate compounds matching FTIR diagram, it can be considered that in FM-FACS there were mainly silicon-containing compounds.

In summary, FACS adsorption materials mainly contain silicate compounds, which are related to the main chemical composition of fly ash. After adsorption of TI-containing wastewater in different systems, the principal chemical bond composition and chemical groups of the adsorption materials do not change.

Chitosan has a strong hydrogen bond within and between molecules, which makes the molecular chain of CS rigid to a certain extent, and then forms a certain crystal shape, which shows an adsorption peak in XRD pattern 2θ in the Angle scanning mode. However, mixing fly ash with CS to make FACS adsorption material would do harm to the crystal shape of CS. The XRD pattern of FACS is illustrated

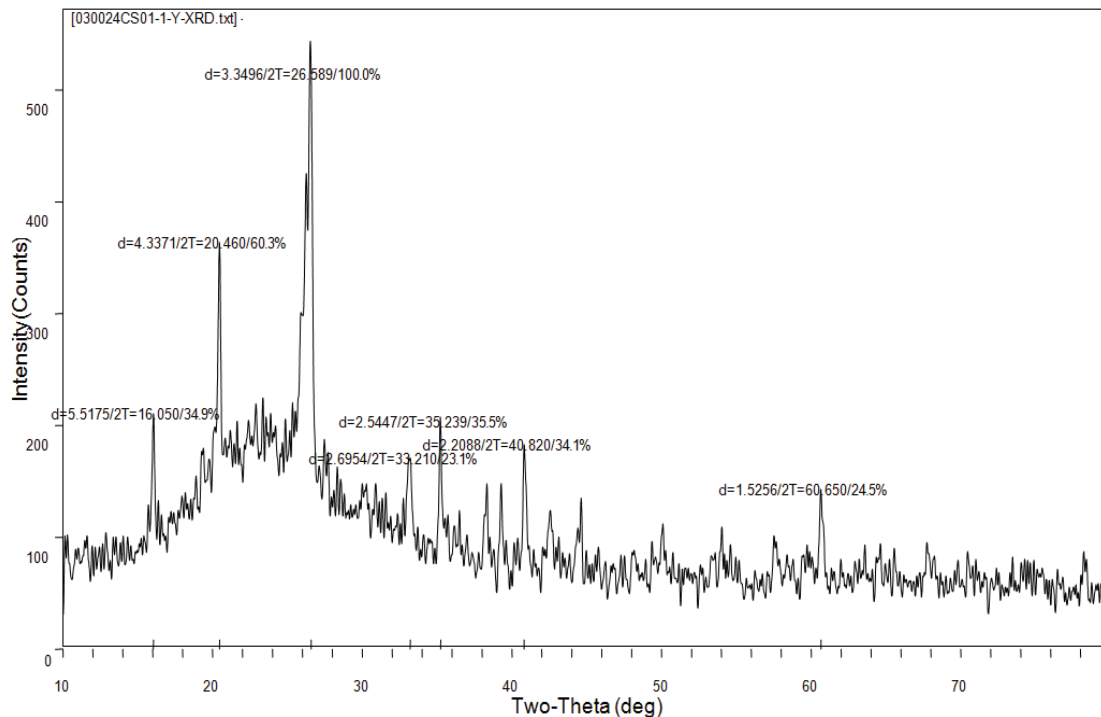


Fig. 3: The XRD picture of FACS.

in Fig. 3, and the diffraction matching pattern is shown in Fig. 4. As can be seen from Fig. 3, FACS exhibited two major diffraction peaks at $2\theta = 20.460^\circ$ and $2\theta = 26.589^\circ$. Compared with the XRD pattern of sillimanite, it is easy to see in Fig. 4 that there were also two distinct diffraction peaks in the XRD pattern of sillimanite at $2\theta=20.456^\circ$ and $2\theta=26.610^\circ$. The matching between the two was extremely high, indicating that the XRD pattern of FACS was a sillimanite map. In the above diffraction pattern, there was no diffraction peak of CS, which indicates that CS would undergo oxidation and substitution reaction with the addition of glacial acetic acid. In addition, after mixing with fly ash, the molecular structure of CS was changed and the crystal form of CS was destroyed. Therefore, only the crystal diffraction peaks of silicon-containing compounds whose crystal forms were not destroyed in the FACS diffraction pattern could be found, which further indicates that the main components of FACS were silicon-containing compounds.

Effect of Solution pH Value on Adsorption

Since the pH value of the solution determines the surface charge of the adsorbent and the degree and shape of the adsorbent, it has a significant impact on the adsorption of heavy metal (Salam et al. 2011). 80mL thallium-containing

wastewater with an initial concentration of 0.010mg/L was loaded into a 250mL conical flask, and 3g adsorbent was added. The same operations were carried in 7 conical flasks, and the pH value of the solution in the flasks was adjusted to 4, 5, 6, 7, 8, 9, 10 with HCl or NaOH, respectively. After shaking at a constant temperature for 2 minutes, the adsorbent was thoroughly mixed with the liquid and permitted to stand for 2 hours, after which the supernatant was taken to determine the TI content. According to the results, the adsorption effect of the adsorbent on TI under different pH conditions was plotted, as shown in Fig. 5.

It is clear that when the pH was 8, the FACS was best for the adsorption of thallium, and the maximum amount of adsorption was 0.173 of $\mu\text{g/g}$. When pH rose from 4 to 6, thallium concentration in the supernatant fluid increased with the increase of pH value, while adsorption capacity decreased gradually, which indicates that in this process, the adsorption effect showed a gradual decline with the increase of pH value. On the contrary, with the pH increasing from 6 to 8, the TI concentration gradually decreased, while the adsorption amount of FACS increased gradually, indicating that the adsorption effect also gradually increased with the increase of pH value. In addition, when the pH was equal to 9 or 10, the concentration of thallium in the solution was consistent with that when the pH was 4

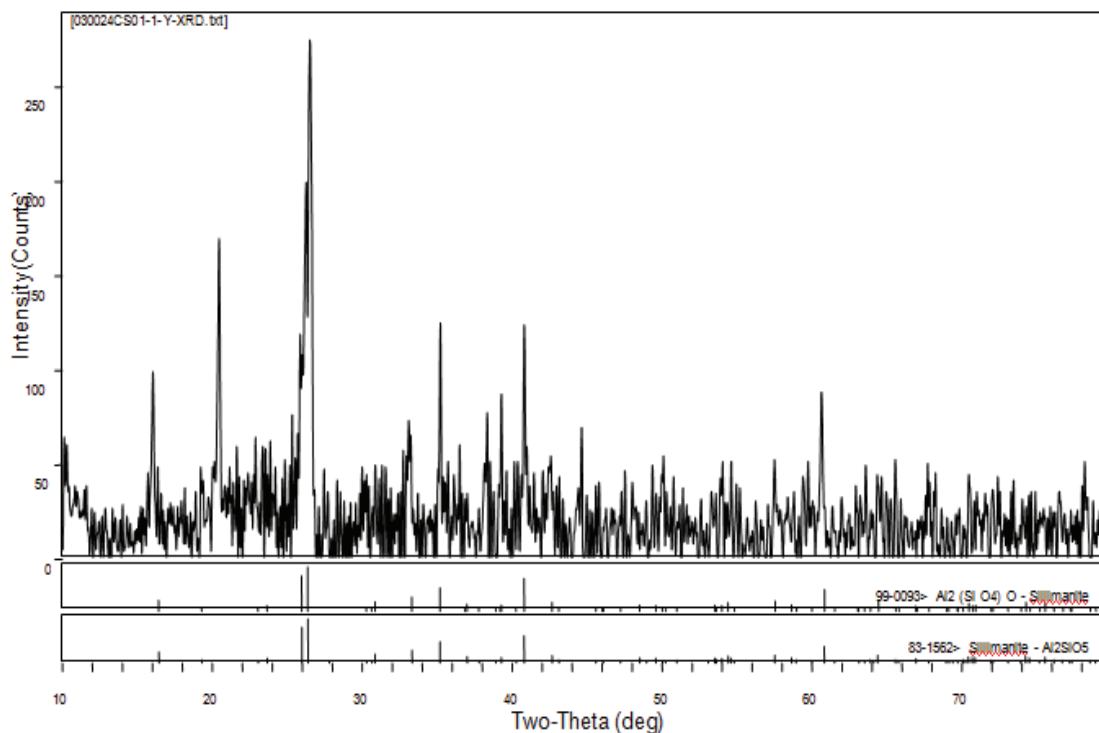


Fig. 4: The matched XRD picture of FACS.

and the concentration was high, and the FACS adsorption amount was small, which means that in an acidic or basic environment, the FACS composite adsorption material was not ideal for the absorption of thallium. At low pH, it could be attributed to the competition between the excessive proton H^+ and the ion metal on the surface of the adsorbent that made the adsorption of TI by adsorbent difficult (Hamadi & Nabih 2018). On the other hand, when the pH value was too high, the adsorption effect of the adsorbent on TI also unsatisfactory, which may be due to more OH^- damaged Si-O bonds of the adsorbent.

Effect of Reaction Time on Adsorption

80mL thallium-containing wastewater with an initial concentration of 0.010mg/L was loaded into a 250mL conical flask, and 3g adsorbent was added respectively, and the same solution pH value was kept. The mixture was shaken at a constant temperature for 2 minutes in order

to thoroughly mix the adsorbent with the liquid, and then the solution was allowed to stand. After 15, 30, 60, 90, 120 and 150 min, the supernatant was taken to determine the content of thallium. The effect of reaction time on adsorption is shown in Fig. 6.

It shows that at the beginning of the adsorption, thallium concentration in the solution decreased with the increase of adsorption time, while the FACS adsorption capacity increased gradually. When the adsorption was carried out for 60 min, the concentration of thallium in the solution reached the minimum, while the adsorption amount reached the maximum, which was 0.182 μ g/g. After the adsorption was conducted for 60 min, the concentration of thallium in the solution gradually increased with the increase of adsorption time, this is because the adsorption has reached saturation. With the increase of adsorption time, the parsing phenomenon began to appear in the solution. It was found that concentration of thallium in

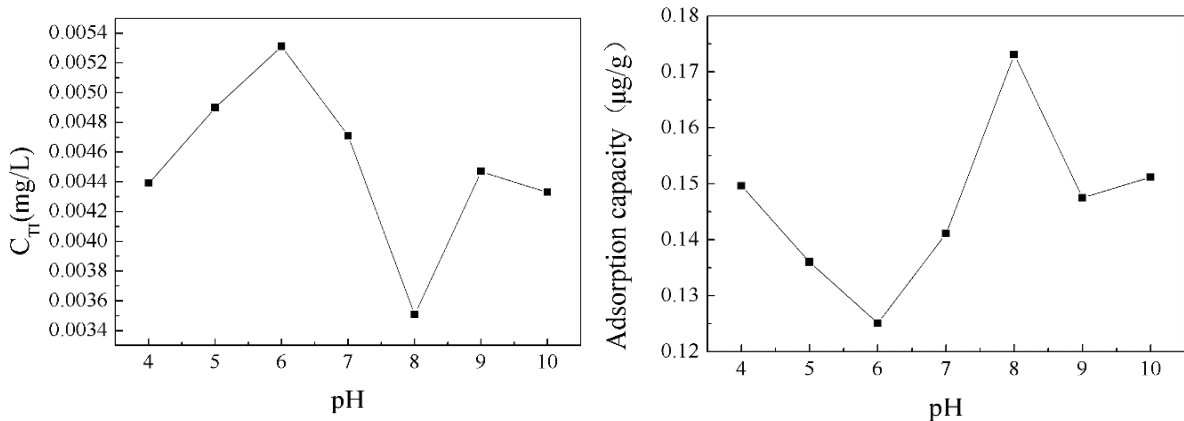


Fig. 5: The effect of solution pH on adsorption.

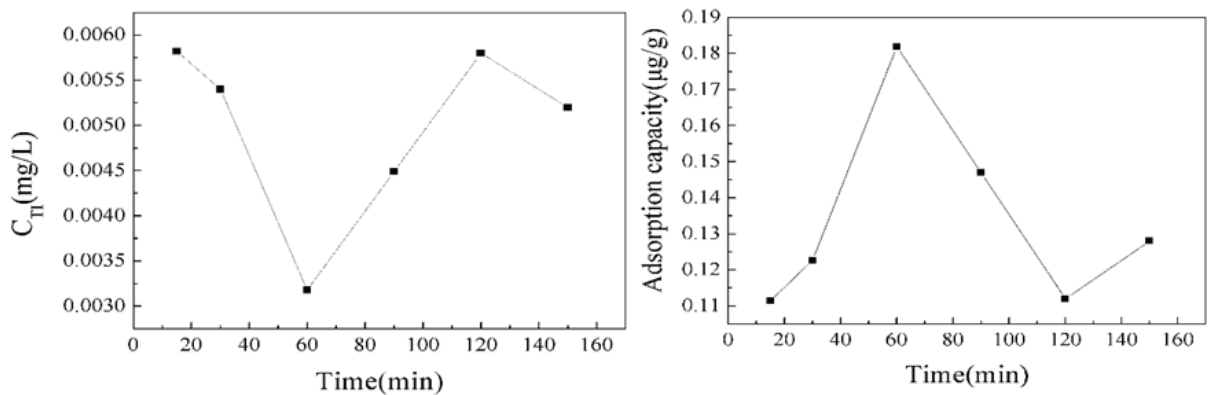


Fig. 6: The effect of reaction time on adsorption.

the solution was reduced again after 120 min, at which point the FACS composite adsorption material resorbed after desorption. Therefore, the reaction of the FACS on the thallium in the wastewater is a kind of adsorption - the alternate process of the absorption cycle. When the reaction time was at 60 min, FACS compound adsorption material reached saturated adsorption, and adsorption effect was best.

Effect of the Amount of Adsorbent on the Adsorption Effect

80mL wastewater containing thallium with an initial concentration of 0.010mg/L was loaded into six 250mL conical flasks, and adsorbents of 1g, 2g, 3g, 4g, 5g and 6g were added, respectively. The pH of the solution was kept same in all the conical flasks, and the solution was shaken at a

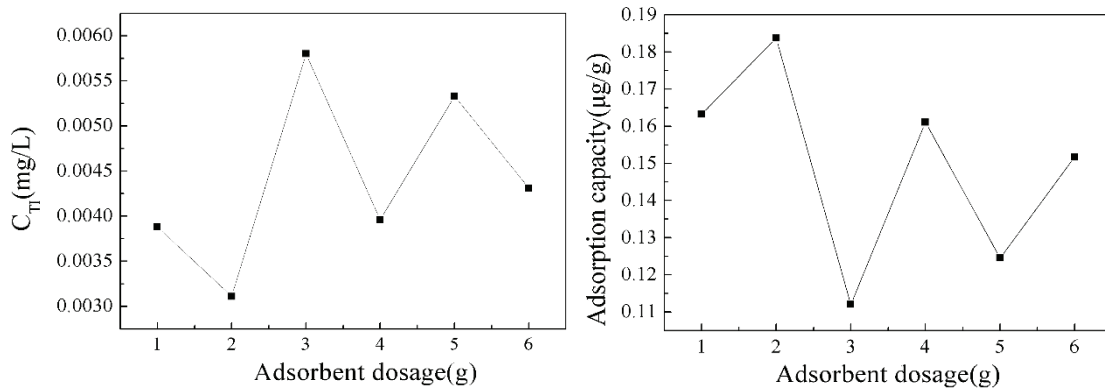


Fig. 7: The effect of adsorbent dose on adsorption.

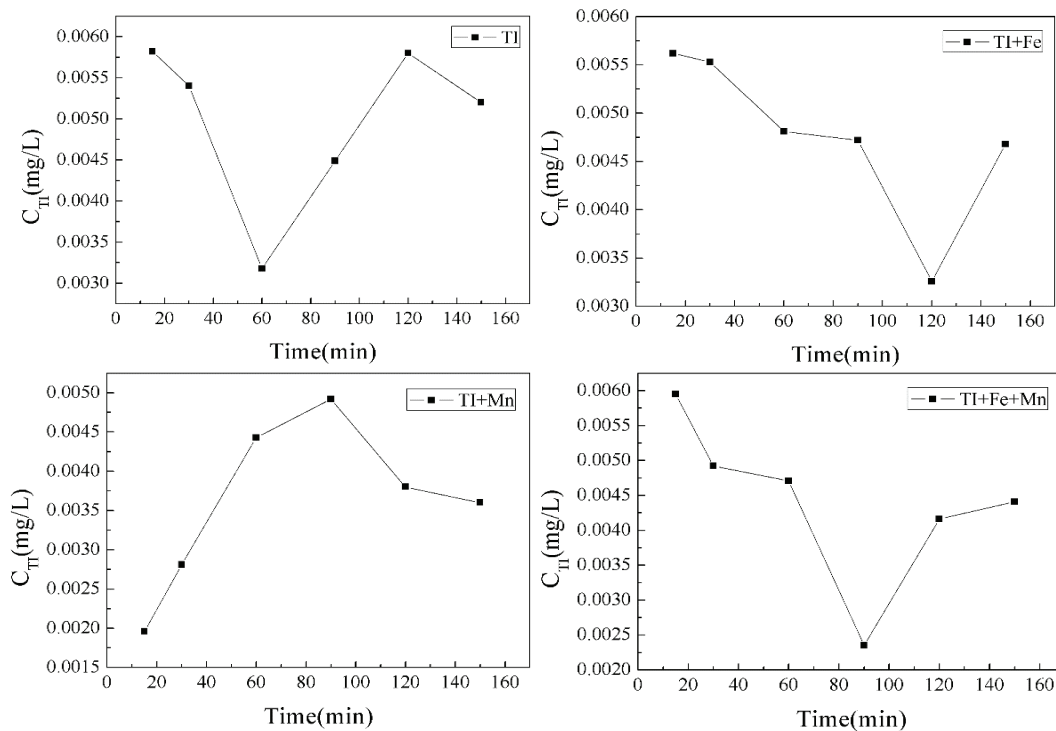


Fig. 8: Variations in the concentration of thallium with time in solutions of different systems in the presence of coexisting ions.

constant temperature for 2 minutes to allow the adsorbent to mix well with the liquid and let it stand. Two hours later, the supernatant was taken to determine the content of thallium, and the results are presented in Fig. 7.

It can be seen directly from the Fig. 7 that by adding the 2g adsorbent, the adsorption quantity of thallium was largest, and adsorbent adsorption effect was best. However, when the amount of adsorbent was more than 2g, the adsorption capacity of thallium by FACS was significantly less than that of the solution with 2g of adsorbent. The reason for this phenomenon may be that when the amount of adsorbent is too much, there would be an adsorption bridge between adsorbent particles, which would affect the adsorption of thallium. On the other hand, the adsorption of thallium may be affected by the intermolecular interaction between ions on the surface of the adsorbent due to the high adsorption dose. In addition, when the amount of adsorbent was less than 2g, the adsorption amount of thallium was also less. Obviously, when the

amount of adsorbent was not enough, the heavy metal thallium in water cannot be fully removed.

Effect of Coexisting Ions on Adsorption

In this study, the effects of Fe^{3+} , Mn^{2+} and $\text{Fe}^{3+}/\text{Mn}^{2+}$ on the removal of TI by FACS were studied respectively. 80mL thallium-containing wastewater with an initial concentration of 0.010mg/L was added into the 250mL conical flask, and 5mL FeCl_3 solution, MnCl_3 solution and $\text{FeCl}_3/\text{MnCl}_3$ mixed solution with a concentration of 0.05mg/L were added, respectively. 3g FACS was added to each conical flask with the same pH value. The conical flasks were shaken so that the solution was fully mixed with the adsorbent. After 15, 30, 60, 90, 120 and 150min, the supernatant was successively taken to determine the content of thallium for analysis. The variations in the concentration of thallium with time in solutions of different systems are illustrated in Fig. 8 and the adsorption amounts of thallium by adsorbent are shown in Fig. 9.

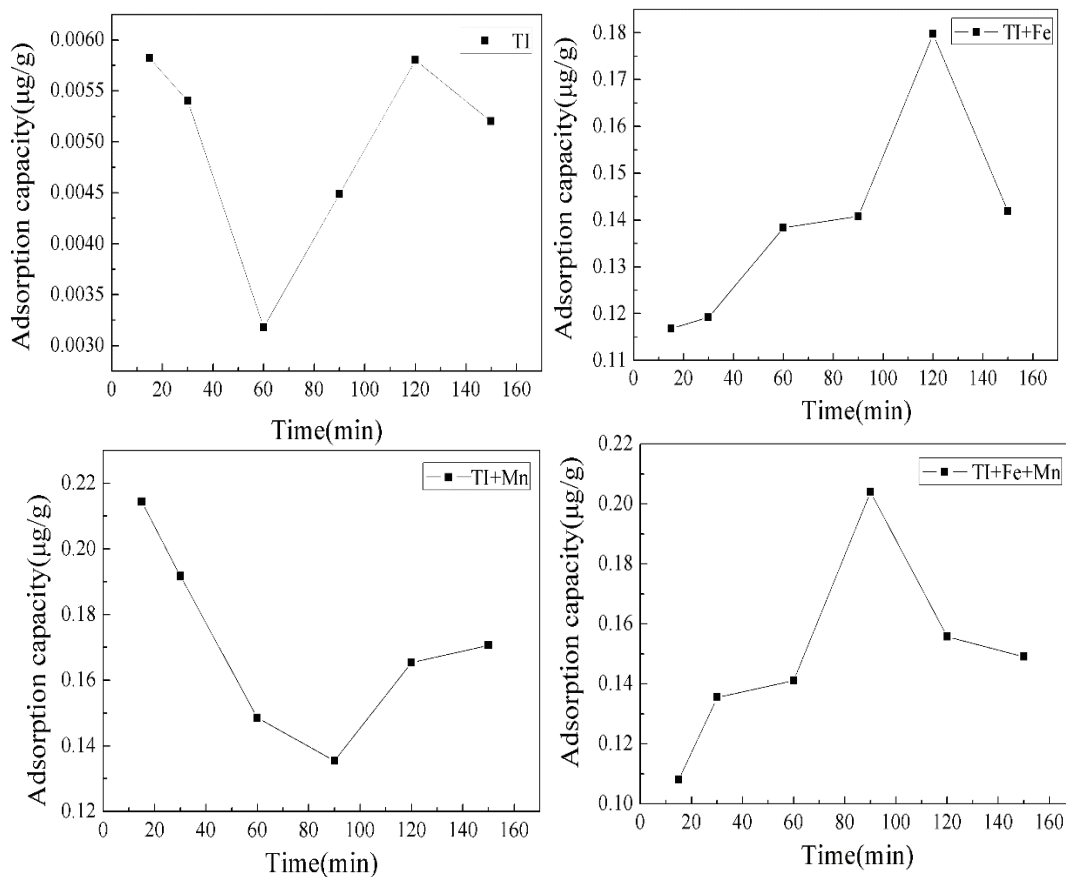


Fig. 9: The variations in the amount of adsorption with time in the presence of coexisting ions.

As can be observed in the figures, when there were no coexisting ions in the solution, the adsorption capacity of FACS on TI increased rapidly between 15 to 60min, and the concentration of TI in the solution decreased significantly. The adsorption saturation was achieved at 60min, and then the concentration of thallium in the solution increased again. When the coexisting ion Fe^{3+} was present, the concentration of thallium in the solution slowly decreases in the first 90min. From 90 to 120min, the adsorption amount increased sharply and the cesium concentration decreased rapidly. At 120min, the amount of adsorption reached its maximum and reached adsorption saturation. Probably due to the presence of the coexisting ion Fe^{3+} , there was competitive adsorption between Fe^{3+} and the TI in the solution for the first 90min of the reaction. When Mn^{2+} was present in the solution, the concentration of strontium in the solution tended to increase continuously between 15 to 90min of the reaction. However, between 90 to 150min, the thallium concentration in the solution showed a trend of gradual decrease. Perhaps Mn^{2+} has a sufficiently strong preferential adsorption capacity over TI, so that the presence of Mn^{2+} seriously disturbed the adsorption behaviour of the adsorbent on TI during the first 90 minutes of the reaction. When TI, Fe^{3+} and Mn^{2+} were present in the solution, the TI concentration in the solution decreased significantly during the first 30 min of the reaction. Between 30 to 60min, the content of TI was still decreasing, but at a slower speed than before. Between 60 to 90min, the content of TI in the solution presented a sharp decline trend again, during which time the adsorption amount of TI by the adsorbent increased significantly. Then, at 90min, the concentration of TI reached the minimum, and the adsorption capacity of the adsorbent on TI was greater than that in the absence of coexisting ions. This is because the fact that Fe^{3+} and Mn^{2+} are hydrolysed to hydroxide.

Except for sediment, they can be used as a new adsorbent to increase the adsorption of TI (Li et al. 2016). After 90 min, the concentration of TI increased in the solution because the FACS reached saturation and desorption occurred.

Effect of Rotation Speed on Adsorption Effect

80mL thallium-containing wastewater with an initial concentration of 0.010mg/L was added into seven 250mL conical flasks. Then 3g adsorbent was added into each flask. Under the same pH, the adsorbent and solution were mixed evenly by shaking. The rotational speed of the thermostatic oscillator was set to 100, 125, 150, 175, 200, 225, and 250r/min, respectively. After the constant temperature oscillation for 120min, the solution was settled and the supernatant was taken to determine the content of thallium in the solution. According to the measurement results, the influence of different oscillation speeds on the adsorption effect of TI was plotted (Fig. 10).

As can be seen, when the rotation speed was 225r/min, the concentration of thallium in the solution was the lowest, and the adsorption amount of the FACS composite adsorbent to TI was the largest. When the rotation speed was between 100 and 175r/min, there was fluctuation in the TI concentration in the solution, but the thallium content in the solution was always higher than that when the rotation speed was 225 r/min, and the thallium content in the solution reached a peak at 175r/min. It may be that the adsorption of TI by FACS adsorbent in the solution is a kind of “adsorption-desorption-re-absorption” alternating complex phenomenon due to the low rotation speed. The adsorption effect of FACS to TI in the second stage was not ideal. At the rotational speed of 175-225r/min, the adsorption amount of TI by FACS increased gradually, while the concentration of TI in the

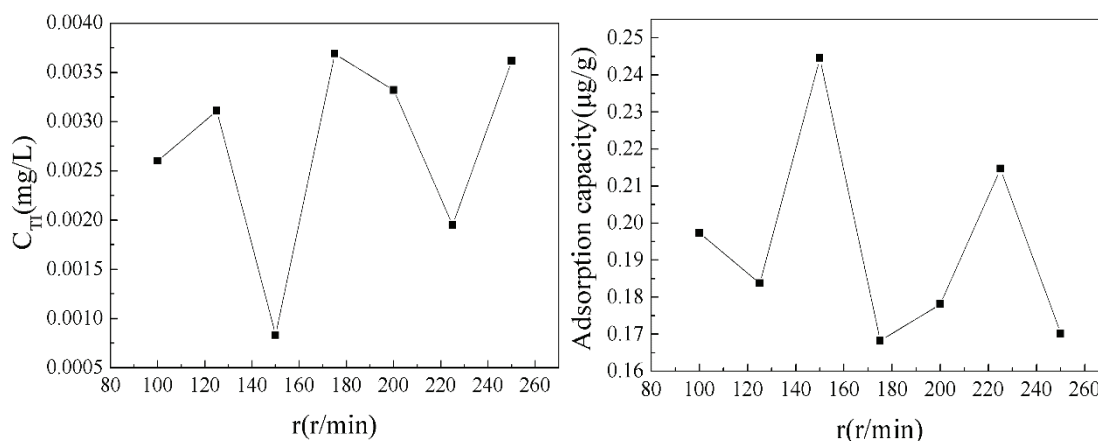


Fig. 10: Influence of different oscillation speeds on thallium adsorption.

solution decreased gradually. However, the thallium concentration in the solution increased sharply as the rotation speed continued to increase. It can be seen that when the speed was too high, severe turbulence was not good for the adsorption of TI in the solution by FACS composite adsorbent.

Adsorption kinetics

In the present study, kinetic sorption data were treated with two simplified kinetic models including First-order kinetics model and Second-order kinetics model. First-order kinetics fitting results are shown in Table 1 and Fig. 11, and the results of Second-order kinetics fitting in Table 2 and Fig. 12.

It is obvious that the second order model fitted better than the first order model, which means chemical adsorption is the main speed limit step.

Adsorption Isotherms

Both Langmuir and Freundlich models were used to fit the adsorption isotherms in this study. The higher regression coefficient (Table 3) indicates that the Freundlich model has better fitting effect on isotherm than the Langmuir model (Fig. 13), which proves that the adsorption of TI (I) by FACS belongs to multi-molecular layer adsorption on heterogeneous phase surface.

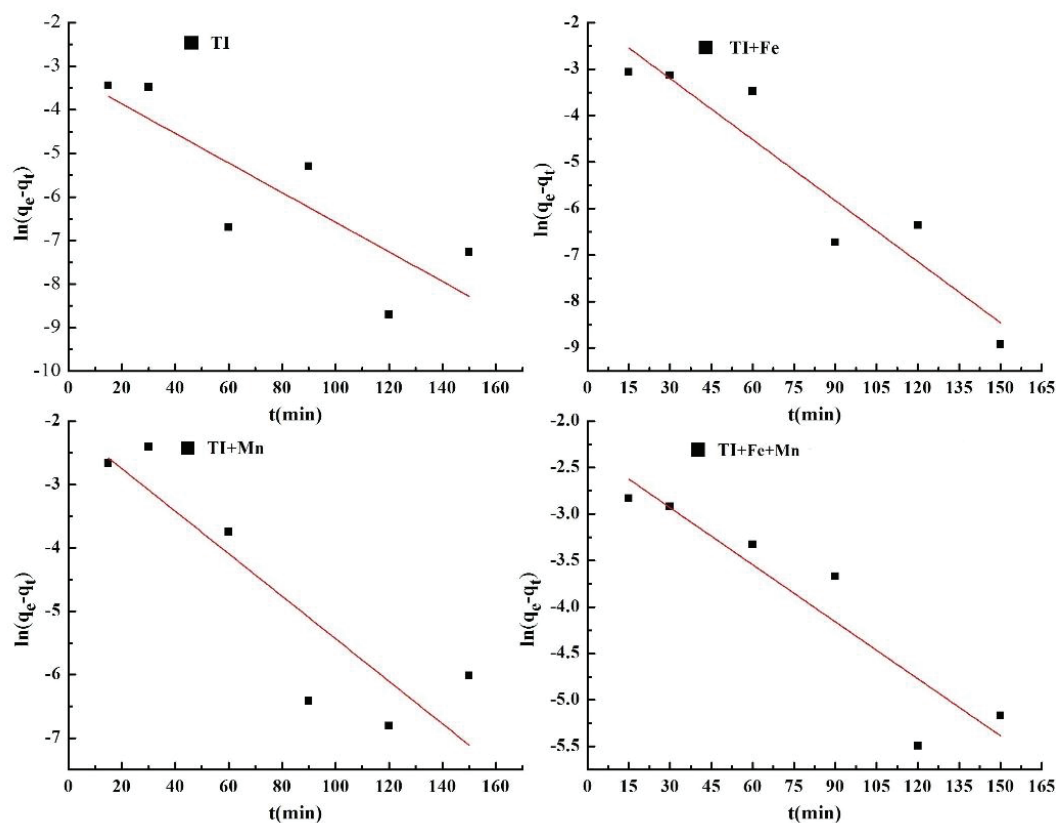


Fig. 11: The First-order kinetic fitting curve.

Table 1: The First-order kinetics fitting parameters.

Reaction system	q_e	q_e^*	k_1	R^2
TI	0.04147	0.17830	0.03397	0.6260
TI+Fe	0.15138	0.20920	0.04379	0.8724
TI+Mn	0.12504	0.22350	0.03355	0.7416
TI+Fe+Mn	0.09855	0.20970	0.02046	0.8302

Table 2: The Second-order kinetics fitting parameters.

Reaction system	q_e	q_e^*	k_2	R^2
TI	0.21589	0.17830	0.65565	0.99903
TI+Fe	0.20648	0.20920	1.05966	0.99238
TI+Mn	0.21206	0.22350	0.45198	0.99222
TI+Fe+Mn	0.21589	0.20970	0.43697	0.99069

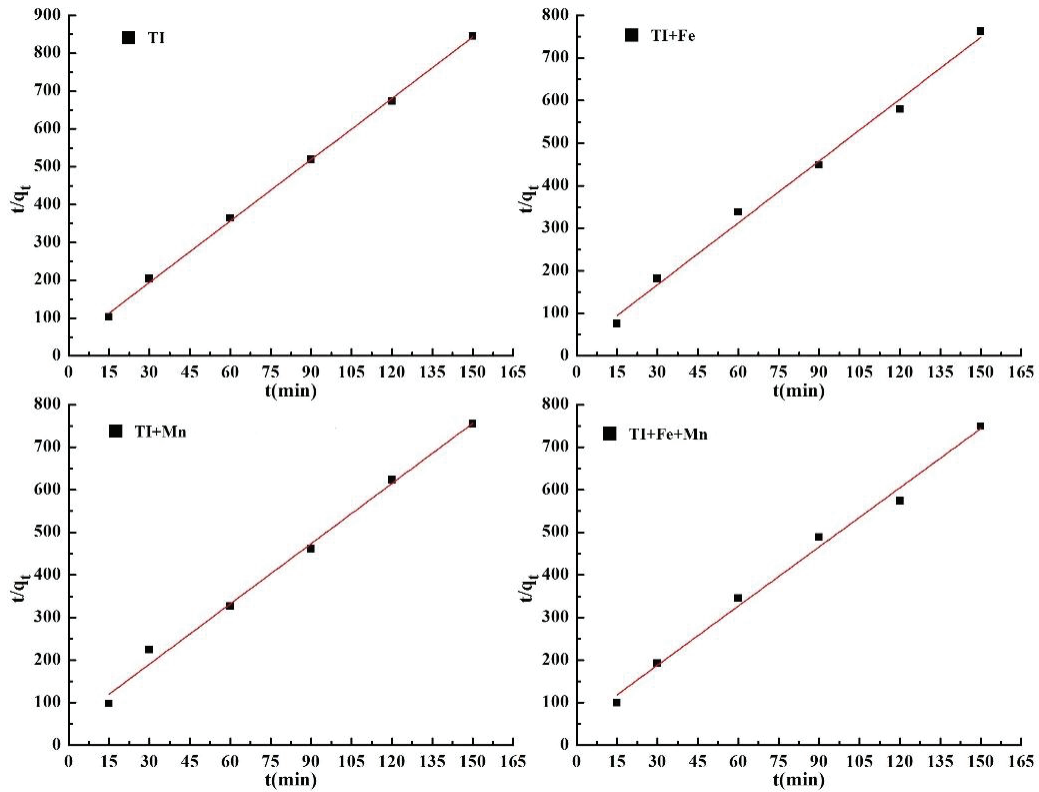


Fig. 12: The Second-order kinetics fitting curve.

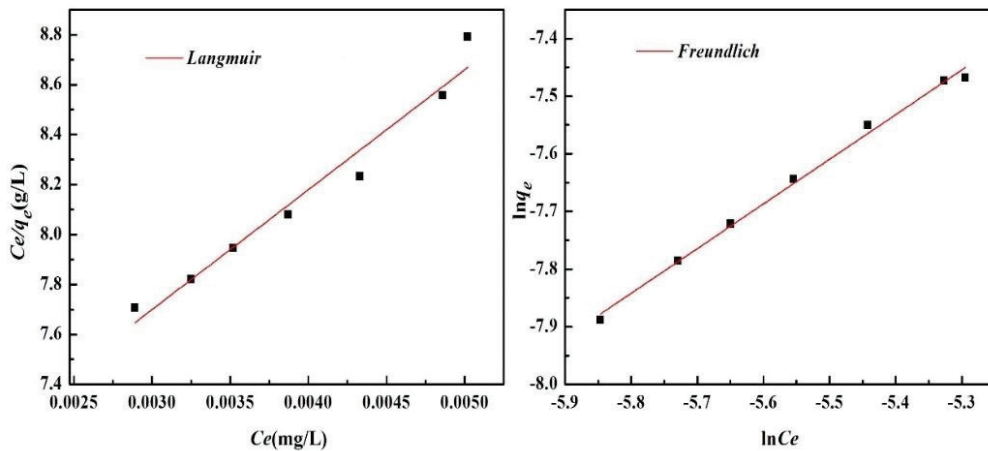


Fig. 13: Isothermal fitting curves of Langmuir and Freundlich.

Reuse of Complex Adsorbent

Because the economy of the adsorption process depends on the regeneration of the adsorbent, the study of desorption is of great importance. The saturated FACS composite adsorbent was repeatedly rinsed with deionized water and then dried. Then, the composite adsorbent was immersed in a sodium chloride solution with a concentration of 1 mol/L for desorption. During the desorption process, the solution was stirred for 1 minute every 2 hours. TI (I) solution was adsorbed by dried FACS for 15, 30, 45, 60, 90, 120 and 150min, respectively. The supernatant was taken in order to measure the concentration of TI (I) in the solution, and the adsorption was calculated. The results are shown in Fig. 14.

Fig. 14 shows that the adsorption step took 60 min to achieve equilibrium and the adsorption capacity was about 0.114 $\mu\text{g/g}$. The removal rate of TI (I) by FACS composite adsorption material reused after desorption was still about 43%, which proves that FACS composite adsorption material still had high activity after regeneration and could be reused in the treatment of TI polluted wastewater. FACS belongs to the adsorption of environmentally friendly materials.

CONCLUSIONS

The prepared FACS composite adsorbent is a low-cost,

renewable, low toxic, environmentally friendly adsorbent material. The surface of FACS particles contains lots of microporous structures and has a large porosity, which is conducive to its adsorption of TI in wastewater. It is mainly of silicate structure. After adsorption of TI-containing wastewater in different systems, the main chemical bond composition and chemical groups of the adsorption material would not change. The experiments of different influencing factors showed that with a pH value of 8, FACS had the best adsorption effect on TI in water. Whether the pH was too high or too low, it had a negative effect on the adsorption. The “adsorption-desorption” period of FACS occurred at 120min, and the adsorption effect was best when the reaction was carried out to 60min, and the adsorption saturation was achieved. When 2g adsorbent was added into 80mL thallium-containing wastewater with an initial concentration of 0.01mg/L, the removal effect was best. When coexisting ions Fe^{3+} and Mn^{2+} were separately present in the solution with TI, both of them had an adverse effect on the removal of TI. However, when Fe^{3+} , Mn^{2+} and TI were simultaneously present in the solution, they had a positive effect on the adsorption. The adsorption effect was optimal when the rotation speed was 225r/min, because the turbulence in the adsorption process is not conducive to the adsorption of TI in the solution by FACS composite adsorbent. The adsorption of TI by FACS was multi-molecular layer adsorption on the surface of heterogeneous reaction. The

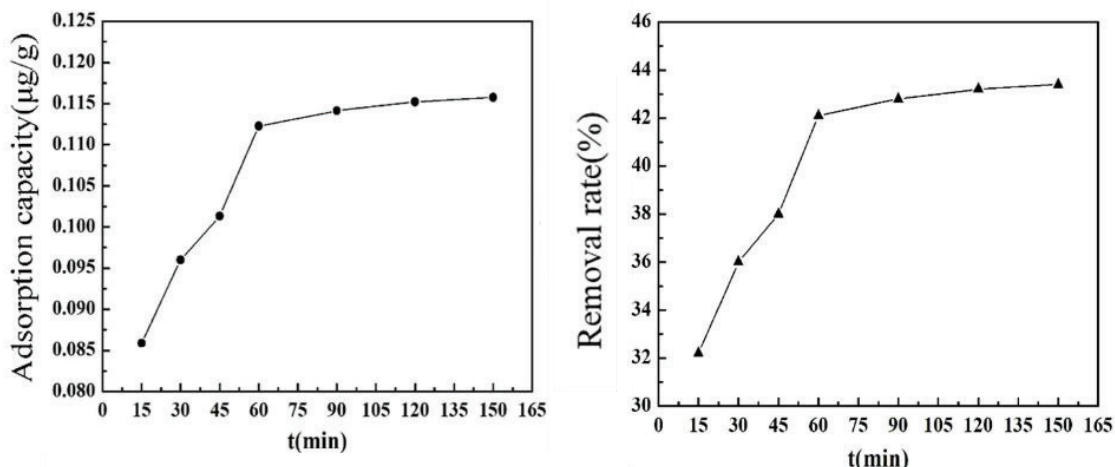


Fig. 14: The change in adsorption capacity and removal rate with time.

Table 3: Langmuir and Freundlich isothermal fitting parameters.

Langmuir isothermal fitting			Freundlich isothermal fitting		
$q_0(\text{mg/g})$	$b(\text{L/mg})$	R^2	n	k	R^2
0.00054	76.60795	0.95820	1.29096	0.03512	0.99438

driving force of the process was the covalent force formed by ion exchange or covalent electron pair between adsorbent and adsorbate. After being analysed and reused, FACS still had superior adsorption efficiency. We believe that FACS composite adsorbent is a kind of economical material with simple operation, low price and recyclability, and has potential application in removing Tl from wastewater.

REFERENCES

- Birungi, Z.S. and Chirwa, E.M.N. 2015. The adsorption potential and recovery of thallium using green micro-algae from eutrophic water sources. *J. Hazard. Mater.*, 299: 67-77.
- Cheam, V., Lechner, J., Desrosiers, R., Sekerka, I., Lawson, G. and Mudroch, A. 1995. Dissolved and total thallium in Great Lakes waters. *Journal of Great Lakes Research*, 21: 384-394.
- Chen, K.N., Li, H.S., Kong, L.J., Peng, Y., Chen, D.Y., Xia, J.R. and Long, J.Y. 2018. Biosorption of thallium (I) and cadmium (II) with the dried biomass of *Pestalotiopsis* sp. FW-JCCW: Isotherm, kinetic, thermodynamic and mechanism. *J. Desalination and Water Treatment*, 111: 297-309.
- Del-valls, T.A., Saenz, V., Arias, A.M. and Blasco, J. 1999. Thallium in the marine environment: First ecotoxicological assessments in the Guadalquivir estuary and its potential adverse effect on the Donana European natural reserve after the Aznalcollar mining spill. *J. Ciencias Marinas*, 25: 161-175.
- Fan, L.L., Luo, C.N., Li, X.J., Lu, F.G., Qiu, H.M. and Sun, M. 2012. Fabrication of novel magnetic chitosan grafted with graphene oxide to enhance adsorption properties for methyl blue. *Journal of Hazardous Materials*, 215-216: 272-279.
- Ge, J.C., Yoon, S.K. and Choi, N.J. 2018. Application of fly ash as an adsorbent for removal of air and water pollutants. *J. Applied Sciences*, 8(7):1-24.
- Hamadi, A. and Nabih, K. 2018. Synthesis of zeolites materials using fly ash and oil shale ash and their applications in removing heavy metals from aqueous solutions. *Journal of Chemistry*, 2018: 1-12.
- Huangfu, X.L., Ma, C.X., Ma, J., He, Q., Yang, C., Zhou, J., Jiang, J. and Wang, Y.A. 2017. Effective removal of trace thallium from surface water by nanosized manganese dioxide enhanced quartz sand filtration. *Chemosphere*, 189: 1-9.
- Keskinkan, O., Goksu, M.Z.L., Basibuyuk, M. and Forster, C.F. 2004. Heavy metal adsorption properties of a submerged aquatic plant (*Ceratophyllum demersum*). *J. Bioresource Technology*, 92(2): 197-200.
- Kuroiwa, T., Takada, H., Shogen, A., Saito, K., Kobayashi, I., Uemura, K. and Kanazawa, A. 2017. Cross-linkable chitosan-based hydrogel microbeads with pH-responsive adsorption properties for organic dyes prepared using size-tunable microchannel emulsification technique. *J. Colloids and Surfaces A: Physicochemical and Engineering Aspects*, 514: 69-78.
- Li, H.H., Yan, W.F., Meng, R.J. and Liang, Q. 2016. Influence of coexistent ions Fe^{3+} and Mn^{2+} on arsenic (iii) adsorption behaviour onto river sediment. *Nature Environment & Pollution Technology*, 15: 305-310.
- Li, H.S., Chen, Y.H., Long, J.Y., Jiang, D.Q., Liu, J., Li, S.J., Qi, J.Y., Zhang, P., Wang, J., Gong, J., Wu, Q.H. and Chen, D.Y. 2017. Simultaneous removal of thallium and chloride from a highly saline industrial wastewater using modified anion exchange resins. *Journal of Hazardous Materials*, 333: 179-185.
- Li, H.S., Li, X.W., Xiao, T.F., Chen, Y.H., Long, J.Y., Zhang, G.S., Zhang, P., Li, C.I., Zhuang, L.Z. and Li, K.K. 2018. Efficient removal of thallium(I) from wastewater using flower-like manganese dioxide coated magnetic pyrite cinder. *J. Chemical Engineering Journal*, 353: 867-877.
- Liu, Y.L., Wang, L., Wang, X.S., Huang, Z.S., Xu, C.B., Yang, T., Zhao, X.D., Qi, J.Y. and Ma, J. 2017. Highly efficient removal of trace thallium from contaminated source waters with ferrate: Role of *in situ* formed ferric nanoparticle. *J. Water Research*, 124: 149-157.
- Memon, S.Q., Memon, N., Solangi, A.R. and Memon, J.U.R. 2008. Sawdust: A green and economical sorbent for thallium removal. *J. Chemical Engineering Journal*, 140: 235-240.
- Pan, J.M., Yao, H., Li, X.X., Wang, B., Huo, P.W., Xu, W.Z., Ou, H.X. and Yan, Y.S. 2011. Synthesis of chitosan/ γ -Fe₂O₃/fly-ash-cenospheres composites for the fast removal of bisphenol A and 2, 4, 6-trichlorophenol from aqueous solutions. *Journal of Hazardous Materials*, 190: 276-284.
- Pu, Y.B., Yang, X.F., Zheng, H., Wang, D.S., Su, Y. and He, J. 2013. Adsorption and desorption of thallium(I) on multiwalled carbon nanotubes. *J. Chemical Engineering Journal*, 219: 403-410.
- Rahmani, A., Mousavi, H.Z. and Fazli, M. 2010. Effect of nanostructure alumina on adsorption of heavy metals. *J. Desalination*, 253(1-3):94-100.
- Rajesh, N. and Subramanian, M.S. 2006. A study of the extraction behavior of thallium with tribenzylamine as the extractant. *J. Hazard. Mater.*, 135: 74-77.
- Rathinam, K., Singh, S.P., Arnusch, C.J. and Kasher, R. 2018. An environmentally-friendly chitosan-lysozyme biocomposite for the effective removal of dyes and heavy metals from aqueous solutions. *J. Carbohydrate Polymers*, 199: 506-515.
- Saad, A.H.A., Azzam, A.M., El-Wakeel, S.T., Mostafa, B.B. and El-latif, M.B.A. 2018. Removal of toxic metal ions from wastewater using ZnO@Chitosan coreshell nanocomposite. *J. Environmental Nanotechnology, Monitoring & Management*, 9: 67-75.
- Salam, O.E. A., Reiad, N.A. and ElShafei, M.M. 2011. A study of the removal characteristics of heavy metals from wastewater by low-cost adsorbents. *Journal of Advanced Research*, 2(4): 297-303.
- Saljooghi, A.S. and Fatemi, S.J. 2011. Removal of thallium by deferasirox in rats as biological model. *Journal of Applied Toxicology*, 31: 139-143.
- Tran, H.N., You, S.J., Hosseini-Bandegharai, A. and Chao, H.P. 2017. Mistakes and inconsistencies regarding adsorption of contaminants from aqueous solutions: A critical review. *J. Water Research*, 120: 88-116.
- Wan, S.L., Ma, M.H., Lv, L., Qian, L.P., Xu, S.Y., Xue, Y. and Ma, Z.Z. 2014. Selective capture of thallium(I) ion from aqueous solutions by amorphous hydrous manganese dioxide. *Chemical Engineering Journal*, 239: 200-206.
- Wen, Y., Tang, Z.R., Chen, Y. and Gu, Y.X. 2011. Adsorption of Cr(VI) from aqueous solutions using chitosan-coated fly ash composite as biosorbent. *Chemical Engineering Journal*, 175: 110-116.
- Wick, S., Baeyens, B. and Fernandes, M.M. 2018. Thallium adsorption onto illite. *J. Environmental Science & Technology*, 52: 571-580.
- Xiao, T.F., Yang, F., Li, S.H., Zheng, B.S. and Ning, Z.P. 2012. Thallium pollution in China: A geoenvironmental perspective. *J. Science of the Total Environment*, 421-422: 51-58.
- Xiong, C.H., Pi, L.L., Chen, X.Y., Yang, L.Q., Ma, C.N. and Zheng, X.M. 2013. Adsorption behavior of Hg^{2+} in aqueous solutions on a novel chelating cross-linked chitosan microsphere. *J. Carbohydrate Polymers*, 98(1): 1222-1228.
- Yang, K., Wang, G., Chen, X.M., Wang, X. and Liu, F.L. 2018. Treatment of wastewater containing Cu^{2+} using a novel macromolecular heavy metal chelating flocculant xanthated chitosan. *J. Colloids and Surfaces A: Physicochemical and Engineering Aspects*, 558: 384-391.
- Zhang, G.S., Fan, F., Li, X.P., Qi, J.Y. and Chen, Y.H. 2018. Superior adsorption of thallium(I) on titanium peroxide: Performance and mechanism. *Chemical Engineering Journal*, 331:471-479.
- Zhang, L., Huang, T., Zhang, M., Guo, X.J. and Yuan, Z. 2008. Studies on the capability and behavior of adsorption of thallium on nano- Al_2O_3 . *J. Journal of Hazardous Materials*, 157: 352-357.
- Zolgharnein, J., Asanjarani, N. and Shariatmanesh, T. 2011. Removal of thallium(I) from aqueous solution using modified sugar beet pulp. *J. Toxicological and Environmental Chemistry*, 93: 207-214.